Mineralogical and radiometric studies of granitic rocks in Wadi Sabbagh area, south Sinai, Egypt

IOP Conf. Series: Materials Science and Engineering **975** (2020) 012018 doi:10.1088/1757-899X/975/1/012018

Mineralogical and radiometric studies of granitic rocks in Wadi Sabbagh area, south Sinai, Egypt

Mira, H. I.[2]., El-Gharbawy, R.I.[1], Elmowafy, A.A.[2], Osman, A.F.[1]and El maadawy, W.M.[2]

[1] Geology Department, Faculty of Science, Ain Shams University, Egypt.
[2] Research sector, Nuclear Materials Authority, Cairo, Egypt.

Abstract. Wadi Sabbagh area is located at southern part of Sinai Peninsula. It is constrained by Latitudes 28° 05′ and 28° 15′ N and Longitudes 34° 00′ and 34° 15′ E. Gneisses, migmatites, metasediments, syn-and post-orogenic granites, in addition to pegmatites and post-granitic dykes are the main rock units encountered in this area. Geological, petrological and geochemical studies indicate that there are two distinct suites of granitoids: older tonalite to granodiorite assemblage and younger two phases (monzo- to syenogranites and alkaline granites). The field radiometric survey and lab investigations indicate that, the anomalous uranium contents are mainly restricted to the pegmatites and altered monzogranites. The eU contents of pegmatites reach up to 168 ppm with an average 117 ppm, while the eTh reach up to 257 ppm with an average 175 ppm. The eTh/eU ratios range from 1.1 to 2.4 with an average 1.6. In the altered monzogranites, eU reachs up to 305 ppm with an average of 126 ppm. The eTh reaches up to 382 ppm with an average of 166 ppm. The average values of Ra and K are 60 ppm and 2.93 wt percentage, respectively. The average values eTh/eU ratios in the examined anomalies monzgranites (1.56) indicating addition of uranium. The high eU and eTh contents may be attributed to the secondary ascending hydrothermal solutions that lead to the accumulation of radioactive mineralizations mostly along fractures, faults and shear districts. The recognized radioactive minerals in the studied pegmatites are thorite, uranothorite, zircon, fluorite, columbite, samarskite, monazite, xenotime and allanite, whereas thorite, uranothorite, zircon and fluorite are the foremost radioactive minerals in the altered younger granites. Additional accessory minerals such as ilmenite, magnetite, hematite, pyrite and rutile were found in the studied pegmatites. Hematite, magnetite and pyrite are the foremost accessories accompanying the radioactive minerals in the altered younger granites.
Keywords. Sabbagh, alkaline granite, monzogranite, pegmatite, dykes, radioactive,hydrothermal solutions.

1. Introduction

Wadi Sabbagh area occupies a part of south Sinai, Egypt figure 1, that featured by the presence of subparallel ridges and low to moderately elevated hills, mostly formed of older and younger granites. Gneisses, migmatites, metasediments, syn- and post-orogenic granites, in addition to pegmatites and post-granitic dykes are the main rock units encountered in this area.

The younger granites, which crop out as elongated belt trending MW-SE and NW-SE directions, occupy about 93% of the total exposed area. Their contacts with all the surrounding rock units are generally sharp and well defined.

The present study deals with field, mineralogy and radioactivity of the younger granites and associated pegmatites in order to identify the radioactive minerals responsible for mineralization.

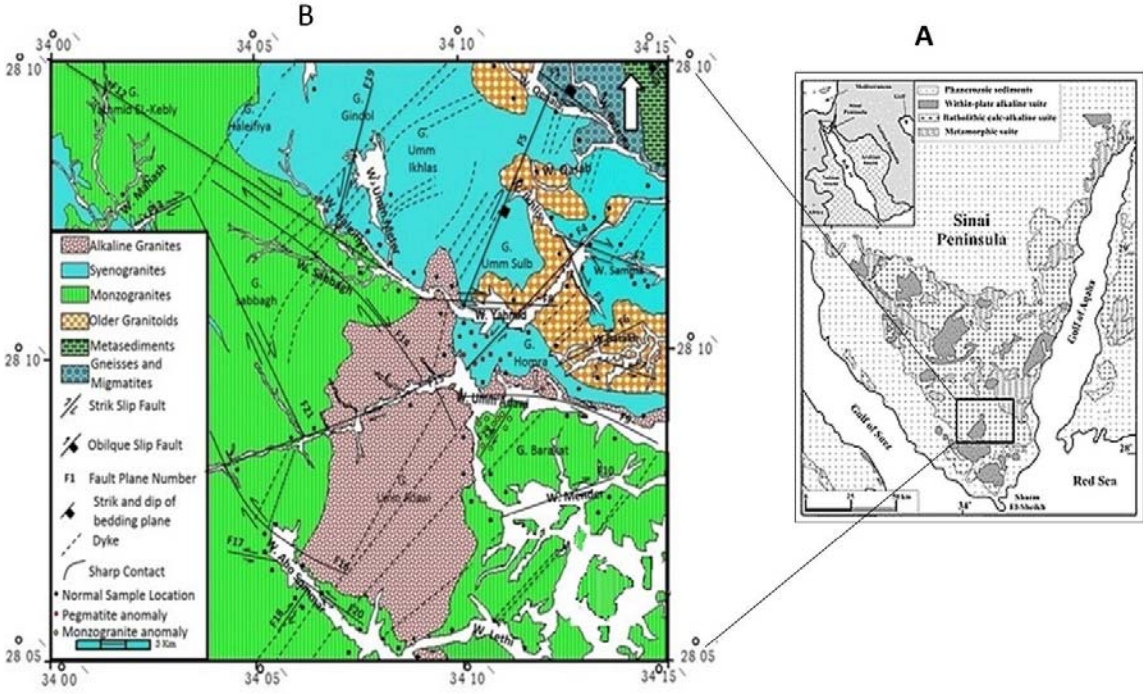

Figure1. A) Simplified geologic map of the late Proterozoic rocks in south Sinai [1] inset a location map of the study area, B) Geologic map of Wadi Sabbagh area, southeastern Sinai, Egypt**.**

2. Methodology

2.1 Field measurements

In situ gamma ray spectrometry measurements have been carried out using a GS-256 spectrometer (designed by Geofyzika Brno-Czech Republic) with a 3" ×3" sodium iodide (Thalium) [NaI (Tl)] crystal detector. The device, having an automatic dead-time correction and an internal ^{137}Cs source allows the spectrometer to automatically maintain system gain stability, is measured over a large body of water. Before field measurements, the spectrometer is calibrated on concrete pads containing known concentrations of U, Th and K. This calibration provides the stripping ratios and sensitivities required for correcting the measured eU, eTh and K.

The measurements are based on the detection of γ-radiation emitted in the decay of ^{214}Bi (^{238}U series) at 1.76 Mev, ^{208}Tl (^{232}Th series) at 2.41 MeV, and the primary decay of potassium ^{40}K (1.46) MeV is measured directly.

The determinations of uranium and thorium are based on the assumption that the daughter nuclides are in equilibrium with the parent nuclides that is none of the intermediate steps in the decay series has been disrupted. Consequently, the deduced amounts of uranium and thorium are equivalent to what would be in equilibrium with the measured radioactivity of the bismuth or thallium isotopes. Therefore, the results of our γ-ray analyses are expressed as equivalent uranium (eU) and equivalent thorium (eTh) [2].

2.2 Lab measurement

Representative grab samples were collected from the studied rocks of Wadi Sabbagh representing the highest values of anomalous field radioactivity. These samples were prepared for gamma-ray spectrometric analysis in order to determine their uranium, thorium, radium and potassium contents by using multichannel analyzer of gamma-ray detector (Gamma-Spectrometer technique). The instrument used in determination of the four radioactive elements consists of a Bicron scintillation detector NaI (Tl) 76x76 mm, hermetically sealed with the photomultiplier tube in aluminum housing. The tube is protected by a copper cylinder protection of thickness 0.6 cm against induced X ray and a chamber of lead bricks against environmental radiation. Uranium, thorium, radium and potassium are measured by using four energy regions representing ^{234}Th, ^{212}Pb, ^{214}Pb and ^{40}K at 93 kV, 239 kV, 352 kV, and 1460 kV for uranium, thorium, radium and potassium, respectively. The measurements were carried out in sample plastic containers, cylindrical in shape, 212.6 cm^3 volumes with 9.5 cm average diameter and 3 cm height. The rock sample is crushed to about 1 mm grain size, and then the container is filled with about 300-400 gm of the crushed sample sealed well and left for at least 21 days to accumulate free radon to attain radioactive equilibrium. The relation between the percentage of ^{222}Rn accumulation and time increase till reaching the steady stage after about 38 days [3]. Mineral separation and identification were carried out at the Laboratories of the Nuclear Materials Authority (NMA). The heavy liquids separation technique using bromoform of specific gravity 2.85 gm cm^{-3} was used to concentrate the heavy minerals. Then, the separation of magnetite was achieved by hand magnet. The heavy mineral fractions were passed through a Frantz isodynamic magnetic to separate the remaining magnetite and produce several magnetic fractions at 0.2, 0.5, 0.7, 1, and 1.5 amperes. Each of these fractions contained its own characteristic minerals. Mineral identification was performed through environmental scanning electron microscope (ESEM) and X-ray diffraction (XRD).

2.3 Field radiometric survey

The field radiometric survey stated that the exhibited rock-units of the studied area are commonly different in their radioactivity concentrations, amongst the granitic rocks, Wadi Umm Adawi monzogranites have the highest radioactive levels, varied between 1000 and 2000 cps. This reveals the function of post magmatic alterations, in addition to fracturing, joints and shearing enriched the radioactivity. The pegmatites exhibit high values of radioactivity (600 to 1200 cps.)

2.4. Lab radioactive survey

2.4.1 Older granites.

The older granites are relatively depleted in eU, eTh, Ra and K contents as compared with the younger granites, the average contents of eU in the tonalite and granodiorite are 3.4 and 5.2 ppm, respectively, whereas the average contents of eTh in these rocks are 8.2 ppm and 11.4 ppm, respectively table 1. All these averages are lower than twice the Clark value (< 8 ppm U and/or 20 ppm Th). The eU content of the two varieties of older granites rest inside the range of acidic intrusives (1-6 ppm) given by Adams et al., 1956 and the low content of K (1.6 and 1.2%) may be related to the low content of K-feldspar minerals in these rocks [4-5].

2.4.2 Younger granites.

Equivalent uranium content ranges from 4-10 ppm in the monzogranites, 5-14 ppm in syenogranites and from 7-15 ppm in alkaline granites (with an average 6.0 ppm, 9.8 ppm and 11.8 ppm, respectively), which are slightly higher than the average of granitic rocks (U; 4 ppm) [6] table 2. On the other hand, the equivalent thorium content of the younger granites varies from 8 ppm to 19 ppm, 11 ppm to 32 ppm and 17 ppm to 28 ppm with an average 13.5, 19.3 and 21.1 ppm for monzogranites, syenogranites and alkaline granites, respectively. The average of thorium content for the studied monzogranites is lesser

than the average of granitic rocks (Th; 19 ppm), whereas syenogranites and alkaline granites average contents are slightly higher than the average of granitic rocks.

Table (1): eU, eTh, Ra and K contents and eU/eTh, eTh/eU and eU/Ra ratios of the studied older granites compared with different local and World averages (10 Samples).

Rock type	Sample no.	eU (ppm)	eTh (ppm)	Ra (ppm)	K%	eU/eTh	eTh/eU	eU/Ra
a)Tonalite	O1	4	11	3	1.95	0.4	2.8	1.3
	O2	3	9	3	1.18	0.3	3.0	1.0
	O3	5	8	4	1.55	0.6	1.6	1.3
	O4	2	5	1	1.47	0.4	2.5	2.0
	O5	3	8	2	1.82	0.4	2.7	1.5
	Average	3.4	8.2	2.6	1.6	0.4	2.5	1.4
b)Granodiorite	O6	4	8	3	1.08	0.5	2.0	1.3
	O7	5	10	4	1.12	0.5	2.0	1.3
	O8	6	13	6	1.07	0.5	2.2	1.0
	O9	3	7	2	1.42	0.4	2.3	1.5
	O10	8	19	7	1.2	0.4	2.4	1.1
	Average	5.2	11.4	4.4	1.2	0.5	2.2	1.2
Older granites of(El Sayed, 1993)		8	17	-	-	-	2.12	-
Older granites of (Sallam, 2006)		2.8	9.3	-	-	-	3.8	-
Older granites of (Abbas, 2008)		3.3	5.8	-	-	-	2.3	-
Acidic intrusive of (Adams et al., 1956)		1-6	1-25	-	-	-	2.6	-

2.4.3 Dykes

The acidic dykes are relatively more enriched in the radionuclides, if compared with the basic dykes. They have eU average content reach up to 9 ppm with an average value 6 ppm, the eTh reaches up to 19 ppm with an average value 12 ppm and the average contents of Ra and K are 5 ppm and 3.7 %, respectively table 3. On the other hand, the average values of eU in the studied acidic dykes show slightly decrease in U contents, but increase in Th contents in comparison with West Dahab area **[7]** and it is in the range of acidic intrusive and effusive given by Adams et al., 1956 [8] table 3.

The field radiometric survey, using γ- gun spectrometry, showed two anomalous zones in the examined pegmatite pockets and veins hosted in syenogranites at the upstream of Wadi Umm Adawi and Wadi Umm Meter, in addition anomalous monzogranites at the downstream of Wadi Umm Adawi figure 1. Thirty representative samples (15 from the pegmatites and 15 from the monzogranites) collected from these regions for the radiometric measurements, table 4 and 5.

Table 2. eU, eTh, Ra and k concentration and eU/eTh, eTh/eU and eU/Ra ratios in the studied younger granites compared with different local and World rocks. (30 samples; 10 monzogranites, 10 syenogranites and 10 alkaline granites)

Rock type	S.N	eU(ppm)	eTh(ppm)	Ra(ppm)	K%	eU/eTh	eTh/eU	eU/Ra
a)Monzogranites	Y1	4	8	2	3.06	0.5	2.0	2.0
	Y2	4	12	5	3.69	0.3	3.0	0.8
	Y3	7	19	5	4.85	0.4	2.7	1.4
	Y4	4	8	3	4.47	0.5	2.0	1.3
	Y5	4	13	6	4.57	0.3	3.3	0.7
	Y6	8	18	5	3.53	0.4	2.3	1.6
	Y7	10	17	4	3.21	0.6	1.7	2.5
	Y8	8	17	4	4.16	0.5	2.1	2.0
	Y9	5	12	5	3.48	0.4	2.4	1.0
	Y10	6	11	5	3.89	0.5	1.8	1.2
	Average	6.0	13.5	4.4	3.9	0.4	2.3	1.5
b)Syenogranites	Y11	7	24	7	3.74	0.29	3.4	1.0
	Y12	5	15	4	4.12	0.33	3.0	1.3
	Y13	14	21	8	4.32	0.67	1.5	1.8
	Y14	10	17	8	3.91	0.59	1.7	1.3
	Y15	12	18	9	4.4	0.67	1.5	1.3
	Y16	8	11	7	3.75	0.73	1.4	1.1
	Y17	8	15	6	3.65	0.53	1.9	1.3
	Y18	9	16	8	4.15	0.56	1.8	1.1
	Y19	11	24	7	3.88	0.46	2.2	1.6
	Y20	14	32	8	3.67	0.44	2.3	1.8
	Average	9.8	19.3	8	3.78	0.53	2.1	1.4
C)Alkaline granites	Y21	15	21	12	3.22	0.35	2.9	1.8
	Y22	12	21	8	4.08	0.57	1.8	1.5
	Y23	10	18	7	4.11	0.56	1.8	1.4
	Y24	16	24	12	3.65	0.67	1.5	1.3
	Y25	8	17	6	4.15	0.47	2.1	1.3
	Y26	7	20	4	4.66	0.35	2.9	1.8
	Y27	9	19	8	3.47	0.47	2.1	1.1
	Y28	17	25	11	4.31	0.68	1.5	1.5
	Y29	11	18	9	3.54	0.61	1.6	1.2
	Y30	13	28	10	3.16	0.46	2.2	1.3
	Average	11.8	21.1	8.7	3.84	0.52	2.0	1.4
Younger granites of (Abbas, 2008)		10.6	27.1	-	-	-	2.3	-
Younger granites of (Sallam, 2006)		7.5	17.5	-	-	-	2.8	-
Granitic rocks of (Rogers and Adams, 1967)		2.2-15	-	-	-	-	-	-
Acidic intrusive of (Adams et al., 1956)		1-6	1-25	-	-	-	2.6	-

Table (3): eU, eTh, Ra and K concentrations and eU/eTh, eTh/eU and eU/Ra ratios in the studied acidic and basic dykes compared with different localities. (11 samples; 8 acidic dykes and 3 basic dykes)

Rock type	Sample no.	eU (ppm)	eTh (ppm)	Ra (ppm)	K%	eU/eTh	eTh/eU	eU/Ra
Acidic dykes	GD1	7	14	5	3.97	0.50	2.0	1.4
	GD2	4	7	3	3.75	0.57	1.75	1.3
	GD3	5	8	4	4.4	0.63	1.6	1.3
	GD4	8	10	5	3.56	0.8	1.3	1.6
	GD5	9	16	7	2.79	0.56	1.8	1.3
	GD6	3	11	2	3.68	0.27	3.7	1.5
	GD7	8	19	6	3.45	0.42	2.4	1.3
	GD8	7	14	5	3.97	0.5	2.0	1.4
	Average	6	12	5	3.70	0.53	2.05	1.4
Basic dykes	GD9	3	2	2	0.68	1.50	0.67	1.5
	GD10	2	5	1	0.95	0.40	2.50	2.0
	GD11	3	7	2	1.79	0.43	2.33	1.5
	Average	3	5	2	1.14	0.78	1.8	1.7
Dykes of El (Sayed, 1993)	Acidic	7	11	-	-	-	1.5	-
	Basic	4	6	-	-	-	1.5	-
Acidic effusiveof (Adams et al., 1956)		2-7	9-25	-	-	-	4.7	-
Acidic intrusive of (Adams et al., 1956)		1-6	1-25	-	-	-	2.6	-
Basic effusiveof (Adams et al., 1956)		0.2-4	0.5-10	-	-	-	3.7	-

2.4.4 Anomalous pegmatites

The anomalous pegmatites are highly enriched in eU, eTh and Ra contents compared to their hosting syenogranites. Their eU content reaches up to 168 with an average of 117 ppm. The eTh content reaches up to 257 with an average of 175 ppm, whereas the Ra content reaches up to 148 with an average of 89 ppm (Table 4). These averages of uranium and thorium contents are higher than those of the world uraniferous pegmatites (av= 28 and 21 ppm for U and Th, respectively) [9]. These averages are also higher than those reported for the Egyptian uraniferous pegmatites (av= 33 and 28 ppm for U and Th, respectively), [10]. The low values of eTh/eU ratios (av = 1.6) of the measured samples suggests that the examined pegmatites are uraniferous [11]. When the average values of both eU and Th in these pegmatites are compared with the average of the Gabal Sheikh El-Arab area, South Sinai, Egypt given by sayed, 1993; Sallam, 2006, the former have lower averages of both eU and eTh table 4.

Table 4. eU, eTh, Ra and K concentrations and eU/eTh, eTh/eU and eU/Ra ratios in the studied anomalous pegmatites compared with different local and World rocks. (15 samples)

Sample no.	eU (ppm)	eTh (ppm)	Ra (ppm)	K%	eU/eTh	eTh/eU	eU/Ra
P1	155	182	76	0.72	0.85	1.2	2.0
P2	90	150	75	3.32	0.60	1.7	1.2
P3	117	153	74	1.6	0.76	1.3	1.6
P4	126	144	94	0.37	0.88	1.1	1.3
P5	168	251	148	1.39	0.67	1.5	1.1
P6	130	156	117	4.09	0.83	1.2	1.1
P7	136	208	121	1.25	0.65	1.5	1.1
P8	123	163	112	3.71	0.75	1.3	1.1
P9	132	178	102	1.75	0.74	1.4	1.3
P10	95	146	69	0.95	0.65	1.5	1.4
P11	111	148	92	0.59	0.75	1.3	1.2
P12	115	169	80	3.86	0.68	1.5	1.4
P13	80	178	67	0.75	0.45	2.2	1.2
P14	114	257	91	0.62	0.44	2.3	1.3
P15	60	141	13	0.65	0.43	2.4	4.6
Average	117	175	89	1.7	0.68	1.6	1.5
Pegmatites of (Sallam, 2006)	157	242.3	-	-	-	1.6	-
Pegmatites of (El Sayed,1993)	162	80	-	-	-	0.49	-

2.4.5 Anomalous monzogranites

The anomalous monzogranite samples at Wadi Umm Adawi area display the greatest values of eU and eTh contents, the eU reachs up to 305 ppm with an average value 126 ppm, the eTh reaches up to 382 ppm with an average value 166 ppm (Table 5). The average values of Ra and K are 60 ppm and 2.93 %, respectively. High eU and eTh contents might be related to the presence of titanite, metamict zircon, opaques, allanite, thorite and uranothorite. The average values eTh/eU ratios in the studied anomalies monzogranites (1.56) exceed those of Sallam, 2006 (0.5) [12] and decrease than those of Abbas, 2008 [13] (4.3), table 5.

Table 5. eU, eTh, Ra and K concentrations and eU/eTh, eTh/eU and eU/Ra ratios in the studied anomalous monzogranites compared with different localities. (15 samples)

Sample no.	eU (ppm)	eTh (ppm)	Ra (ppm)	K%	eU/eTh	eTh/eU	eU/Ra
GR1	305	285	127	0.86	1.07	0.93	2.4
GR2	66	126	50	1.22	0.52	1.9	1.3
GR3	94	109	76	2.16	0.86	1.16	1.2
GR4	228	175	63	5.41	1.3	0.77	3.6
GR5	261	195	58	2.46	1.34	0.75	4.5
GR6	251	382	100	1.87	0.66	1.52	2.5
GR7	55	94	29	2.15	0.59	1.71	1.9
GR8	77	235	65	5.09	0.33	3.05	1.2
GR9	130	100	74	1.67	1.3	0.77	1.8
GR10	75	163	68	2.82	0.46	2.17	1.1
GR11	28	31	14	5.88	0.9	1.11	2.0
GR12	41	60	20	2.59	0.68	1.46	2.1
GR13	21	37	8	5.59	0.57	1.76	2.6
GR14	165	188	93	1.67	0.88	1.14	1.8
GR15	97	315	54	2.52	0.31	3.25	1.8
Average	126	166	60	2.93	0.78	1.56	2.1
Anomalous granites of (Abbas, 2008)	376.3	1624.7	-	-	-	4.3	-
Anomalous granites of (Sallam, 2006)	65.3	31.3	-	-	-	0.5	-

3. Results and Discussions

3.1. eU vs eTh

Figure 2, shows moderately positive correlation for older, younger granites and acidic dykes, while anomalous monzogranites and anomalous pegmatites show moderately to weak positive correlation between eU and eTh figure 2, indicating that the magmatic processes played an important role in the concentration of the radioelements in these rocks.

3.2. eU vs eU/eTh

The eU-eU/eTh variation diagram figure 3 clarifies that the eU/eTh ratios increase with increasing eU content, suggesting post magmatic redistribution of uranium [14], the older, younger granites and acidic dykes display weak positive correlation, while both anomalous pegmatites and monzogranites illustrate moderately positive correlation.

3.3. eTh vs eU/eTh

The eTh and eU/eTh binary relation figure 4 exhibit negative correlation, proposes that the distribution of uranium and thorium remained is partly controlled by magmatic processes, [14 and 15].

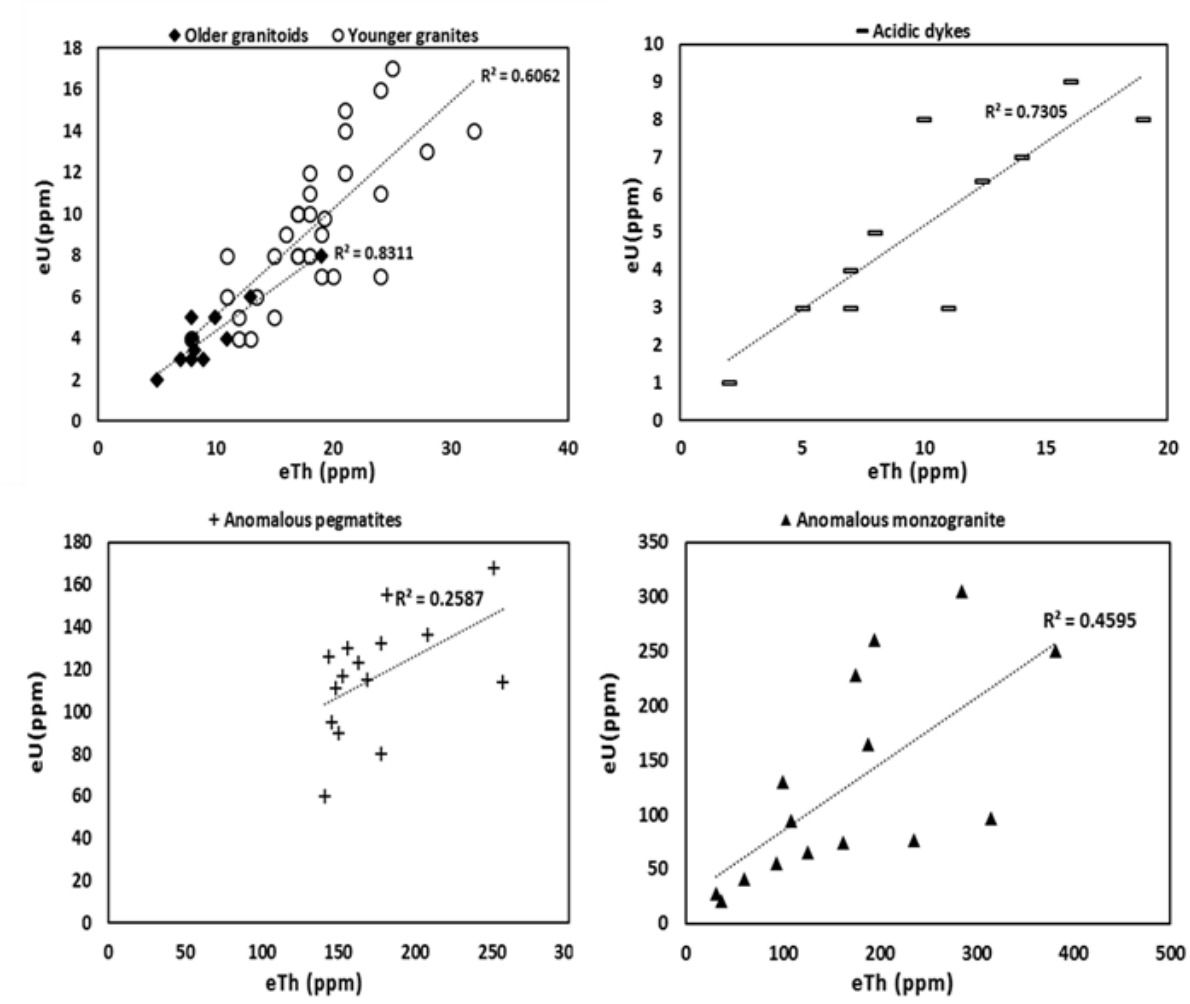

Figure 2. Variation diagrams of eU vs eThin studied rock samples.

3.4. eU vs K

The eU-K variation diagram shows scatter relationship between the eU and K designates the redistribution and mobilization of uranium [14]. This variety of the inter-elements relationship recommends that the radioactivity could be linked to syngenitic and epigenetic processes.

3.5. Mineralogical studies

The mineralogical studies are carried out on some representative samples of the mineralized uraniferous pegmatite and monzogranite. These samples have high uranium and/or thorium.

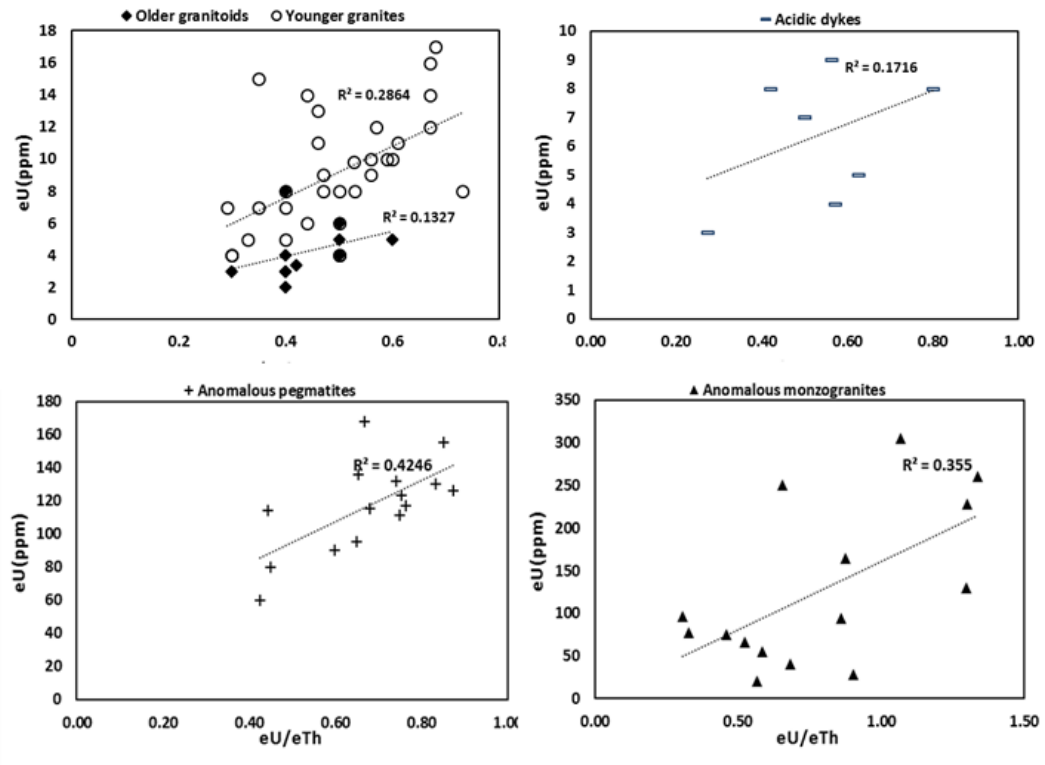

Figure 3. Variation diagrams of eU vs eU/eTh in studied rock samples.

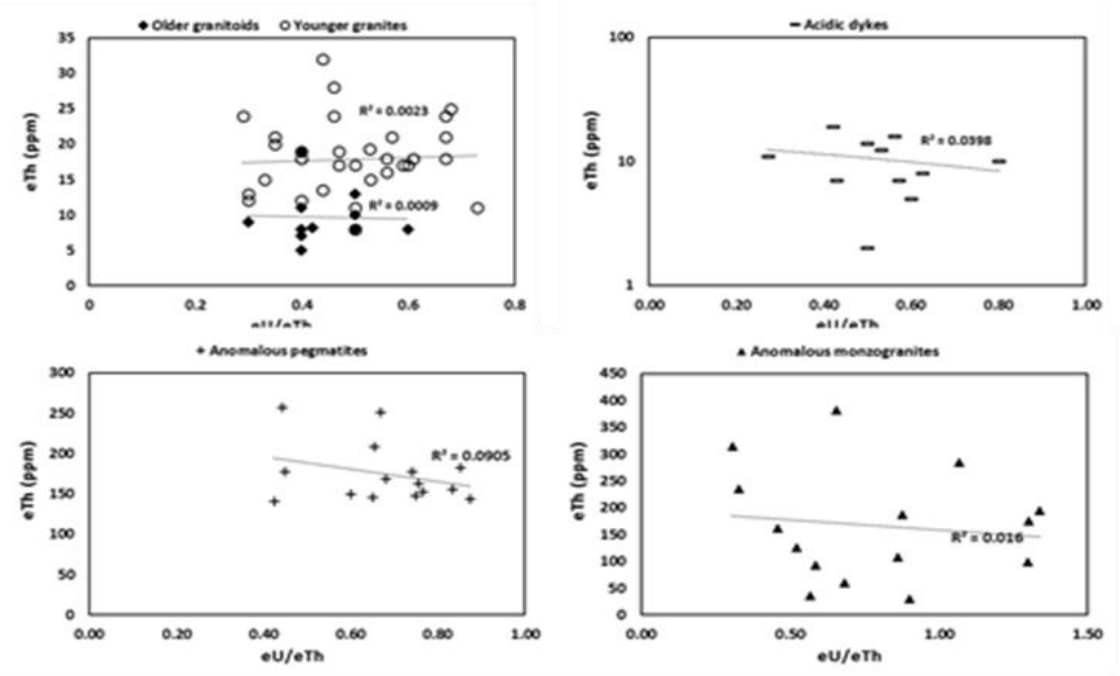

Figure 4. Variation diagrams of eTh vs eU/eThin studied rock samples.

contents. Twenty-one radioactive samples selected for mineralogical studies. The identification of the heavy minerals in these fractions carried out using X-ray diffraction (XRD) and scaning electronic microscope (SEM) technique

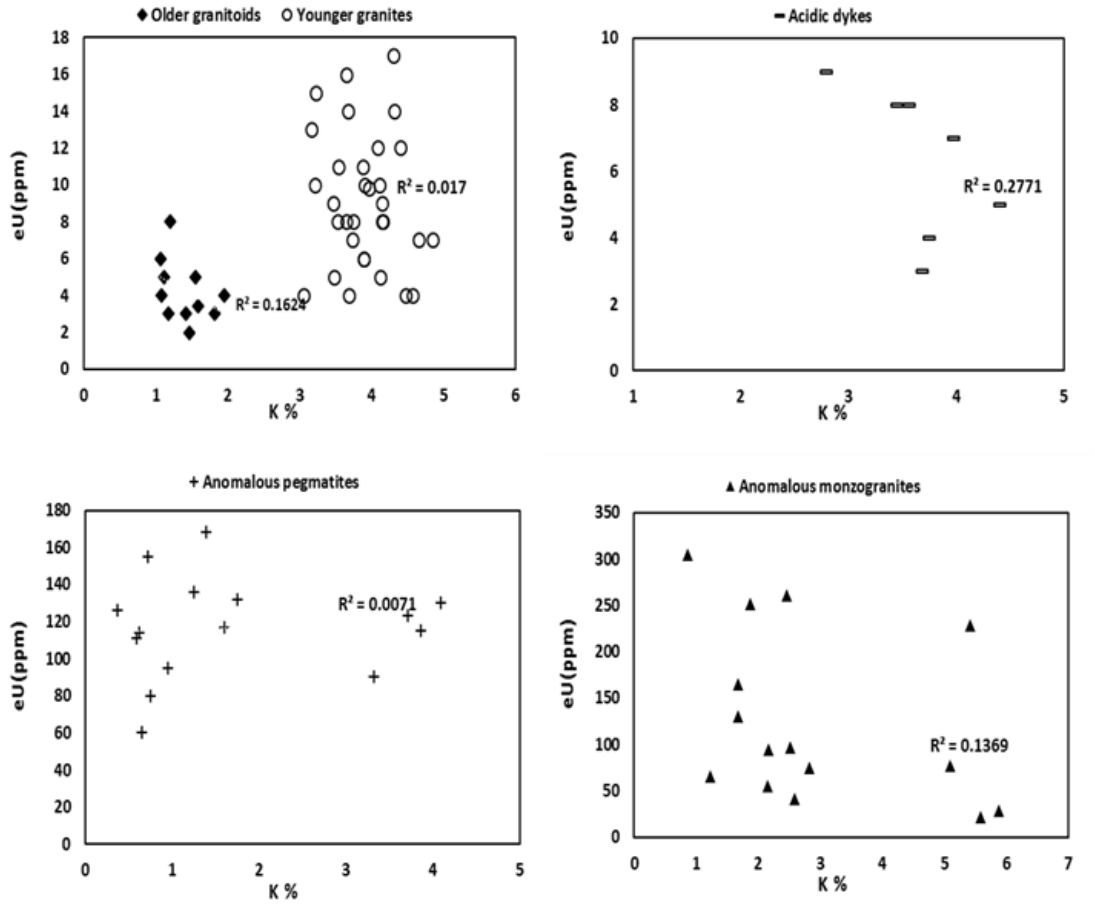

Figure 5. Variation diagrams of eU vs K in studied rock samples.

The data of both XRD and EDX analyses manifested the presence of significant radioactive minerals in assosciätion with non-radioactive ones. The identified radioactive minerals in the anomalous pegmatites are thorite, uranothorite, zircon, fluorite, columbite, samarskite, monazite, xenotime and allanite. However, thorite, uranothorite, zircon and fluorite are the main radioactive minerals in the anomalous monzogranite samples. Other accessory minerals such as ilmenite, magnetite, hematite, pyrite and rutile were identified in the studied pegmatite. On the other hand, hematite, magnetite and pyrite are the foremost accessories accompanying the radioactive minerals in the anomalous monzogranites.

3.6. *Radioactive Minerals*

Thorite [$ThSiO_4$] mineral grains noted in the pegmatites and in the monzogranites, appears as subhedral to anhedral form varying in colour from brownish black to black with greasy luster figure 6A. figure 6B showed the XRD patttern of picked separated grains of thorite and were also confirmed by EDX analyses which reflecting the chemical composition of thorite figures. 7 and 8.

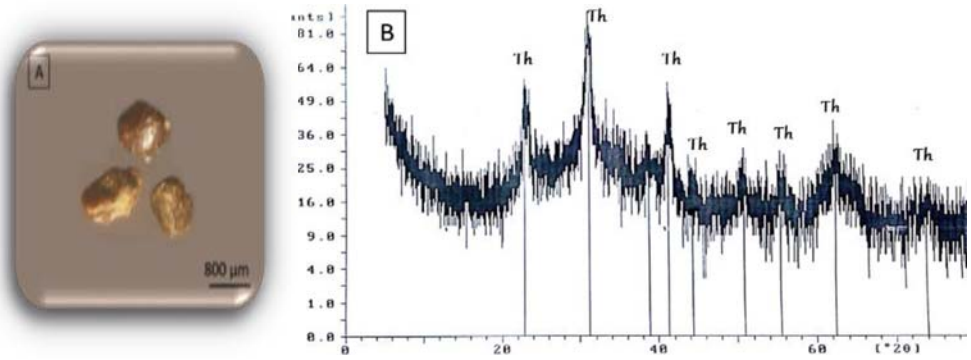

Figure 6. Photomicrograph of thorite grains(A) and X-ray diffraction pattern of thorite (B).

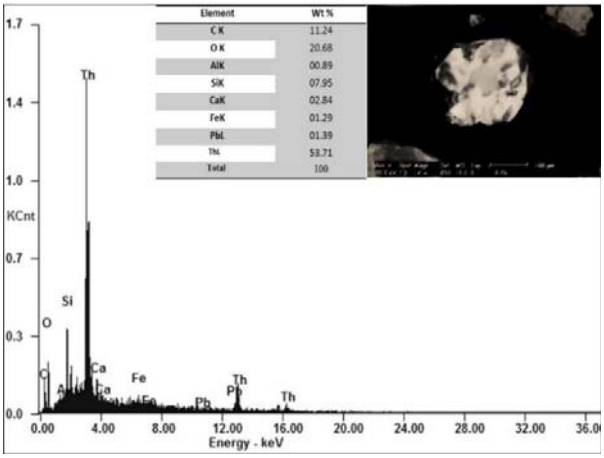

Figure 7. EDX analysis and BSE image of thorite in pegmatite.

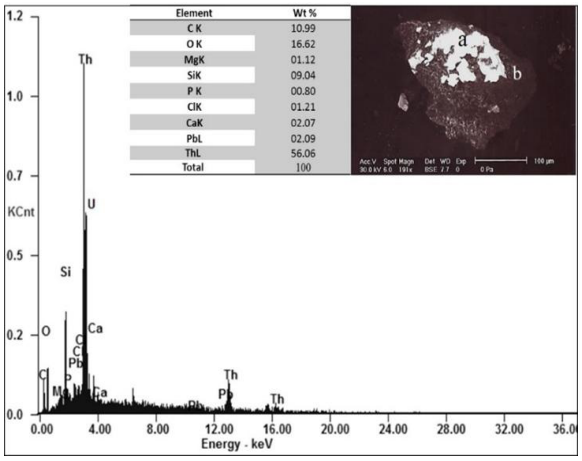

Figure 8. EDAX and BSE image shows inclusion of thorite (a) in flourite grain (b), anomalous monzogranite.

Uranothorite[$(U,Th)SiO_4$] is noted as subhedral to anhedral grains in the pegmatites, yellowish brown to brown with vitreous and resinous luster figure 9, and found in the monzogranites as inclusions in zircon and flourite. The uranothorite grains are highly metamicted, due to crystal lattice annihilation resulting from the influence of its own radioelement contents. Occasionally, the influence of this metamictization destroy the crystal lattice completely but leave the outward appearance unchanged. The existence of Y and P may assign to the assosciation of xenotime as solid solution with uranothorite, the obtained EDAX spectrum figures 10 and 11 reveals the chemical composition of uranothorite.

Figure 9. Photomicrograph of uranothorite grains.

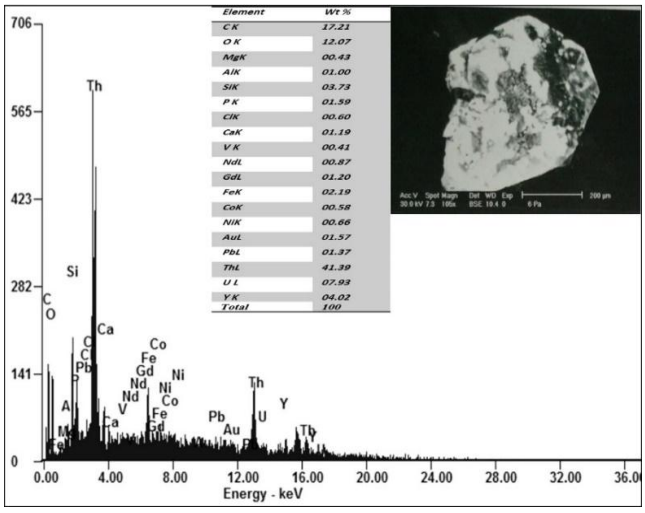

Figure 10. EDAX and BSE image shows uranothorite, pegmatite.

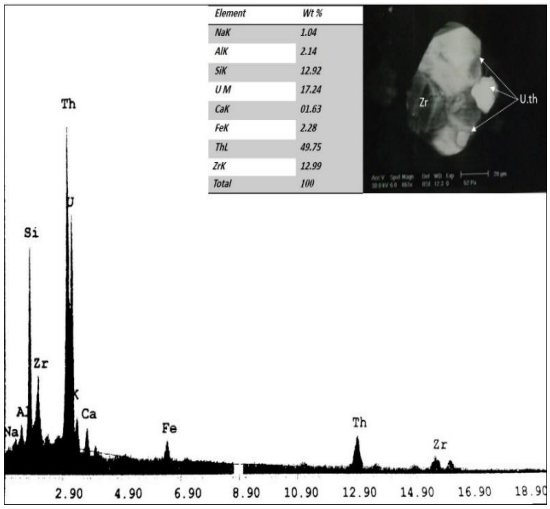

Figure 11. EDAX and BSE image shows uranothorite in zircon grain, anomalous monzogranite.

3.7. Radioelements-bearing minerals

Zircon [$ZrSiO_4$] is the most widespred mineral in pegmatite and anomalous monzogranite, it forms euhedral to anhedral prismatic grains, characterized by bipyramidal ends, varying in colour from yellow, yellowish red to reddish brown and sometimes has colorless to pale yellow colors figure 12. The X-ray diffraction pattern confirms that the picked zircon grains match with the ASTM card No. (6-0266) figure 12E. Also, Scanning Electron Microscope analyses carried out on particular zircon mineral grains picked from pegmatites and alterd younger granites, the back scattered electron microscope images of euhedral zircon grains and the EDX analyses confirm zircon composition [16] figure 13.

Fluorite[CaF_2] is found in all rock units especially in fluorite-bearing quartz vein cutting Gabal Homra pegmatite and Gabal Barakat monzogranite, the seperated grains appear as euhdral to subhedral cubic crystals, varying in colour from colorless to violet and occasionally black in pegmatites (Figures 14A and B) and colorless to deep violet with vitreous luster in altered younger granites figures 14C and D. The X-ray diffraction pattern displays that the picked fluorite grains match with the ASTM card No. (4-864) figure 15. On the other hand, Environmental Scanning Electron Microscope (ESEM) analyses match the chemical composition of fluorite figures 16 and 17.

Columbite [(Fe, Mn) Nb_2O_6] verified in the studied pegmatite by using ESEM analyses. It is characterized as blackish to dark brown prismatic crystals figures 18. Semiquantitative analyses display that columbite has prominent Nb/(Nb+Ta) and could be classed as ferrocolumbite in expression of quadrilateral end members; $FeNb_2O_6$, $MnNb_2O_6$ and $MnTa_2O_6$. The U-bearing columbite is Ta poor figure 19.

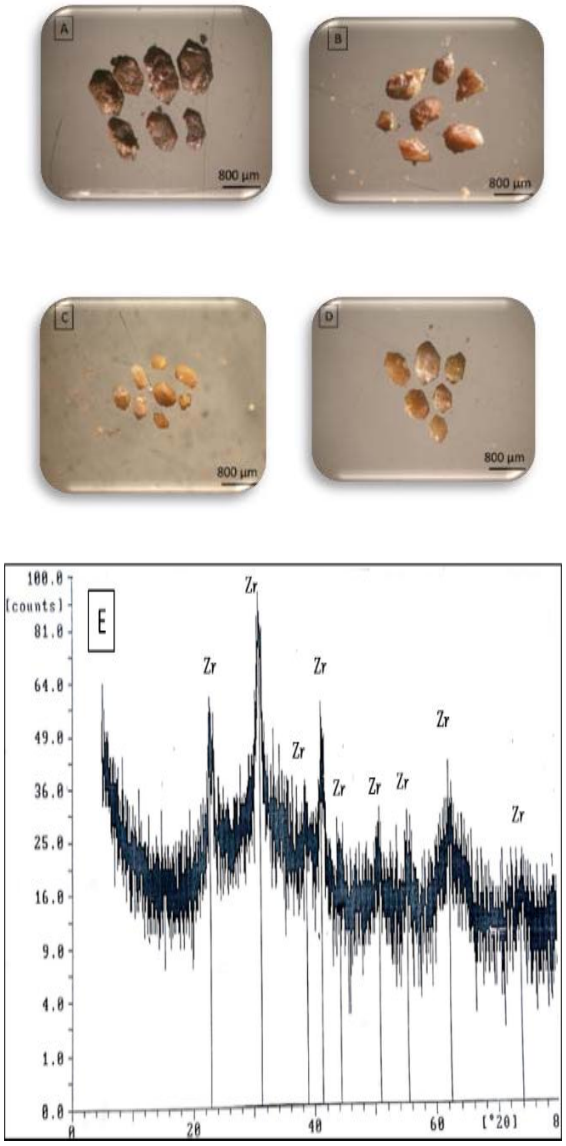

Figure 12. Photomicrographs of zircon grains from pegmatite (A&B), anomalous monzogranite (C&D)and X-ray diffraction pattern (E).

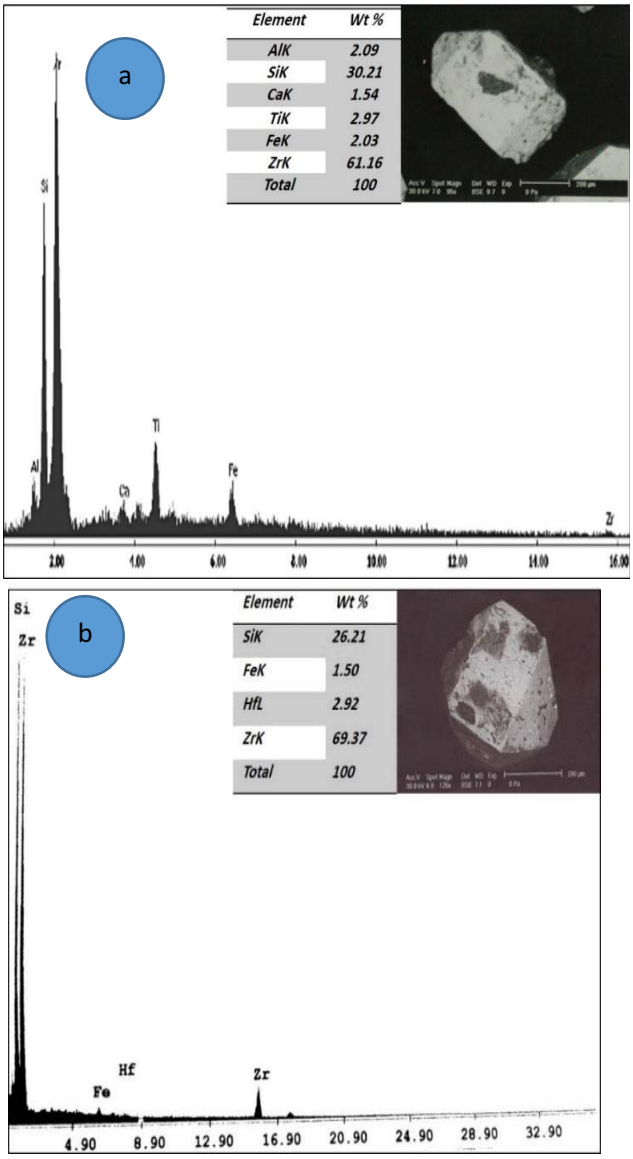

Figure 13. ESEM analyses of zircon grains, pegmatites (a) and anomalous monzogranite (b).

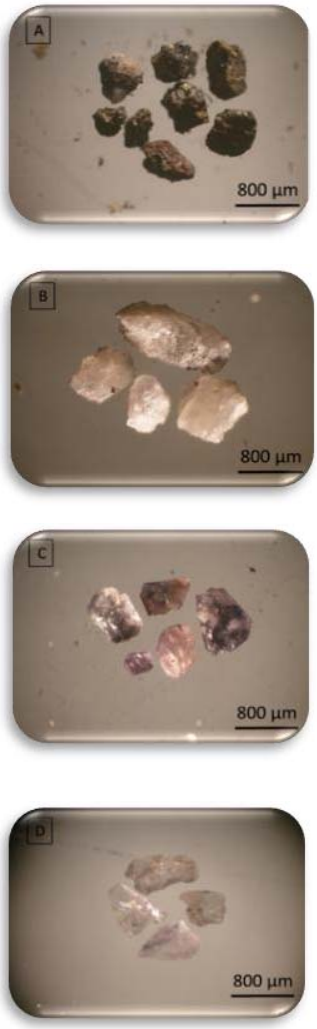

Figure 14. Photomicrographs of flourite grains from pegmatite (A&B),anomalous monzogranite (C&D).

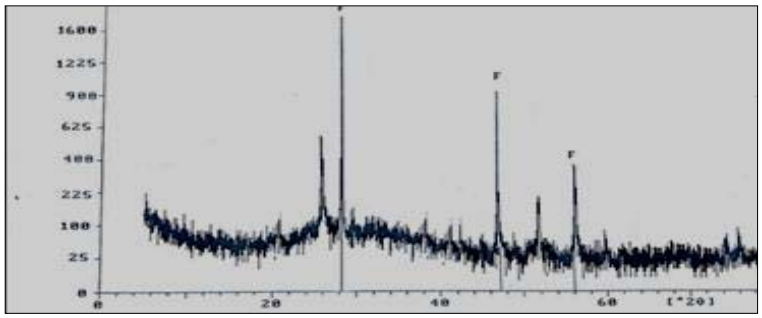

Figure 15. X-ray diffraction pattern of flourite grains, pegmatites (E).

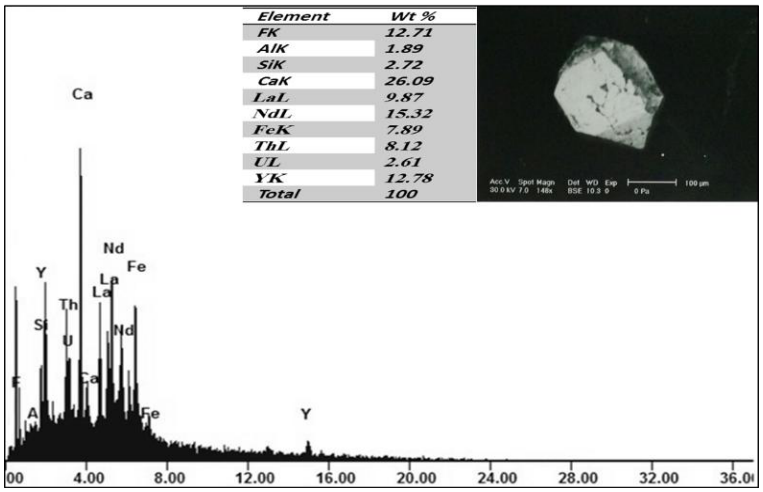

Figure 16. ESEM analyses of flourite grain, pegmatites

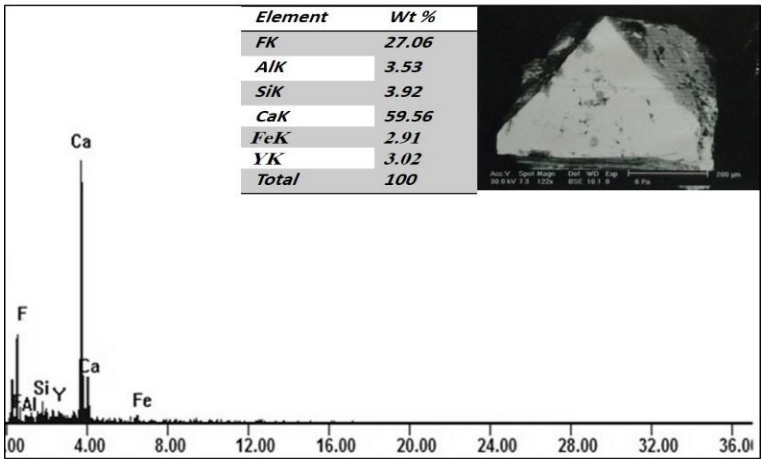

Figure 17. ESEM analyses of flourite grain, altered younger granites .

Figure 18. Photomicrograph of columbite grains, pegmatite.

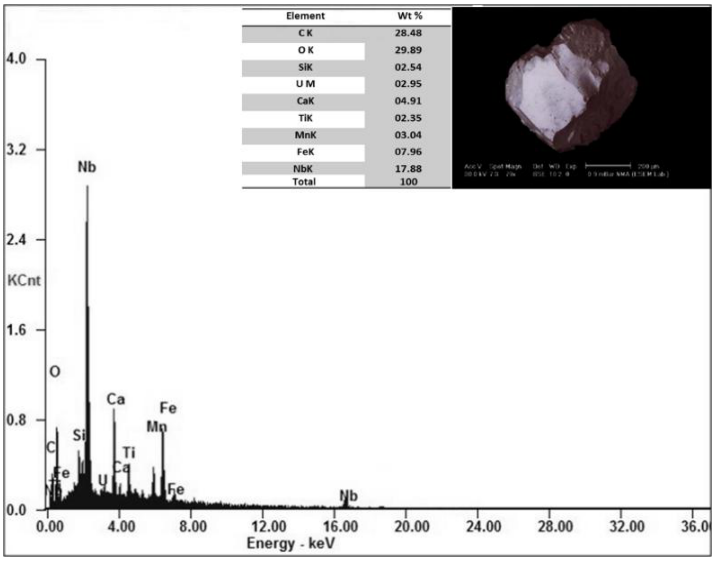

Figure 19. ESEM analyses of columbite grain, pegmatite.

Samarskite $\{(Y,Er,HRE)_4[(Nb,Ta)_2O_7]_3\}$ grains occur as granular massive crystals of reddish orange color (Fig. 20). The recognized mineral is confirmed by ESEM analysis, also the acquired semi quantitative analysis demonstrate that this mineral is chiefly composed of Nb, Th, U, Y, Ca Ti, Ta in addition to REEs figure 21.

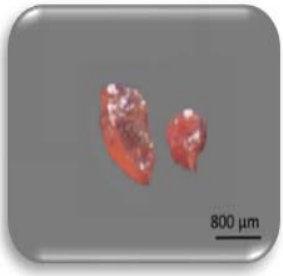

Figure 20. Photomicrograph of samarskite grains, pegmatite.

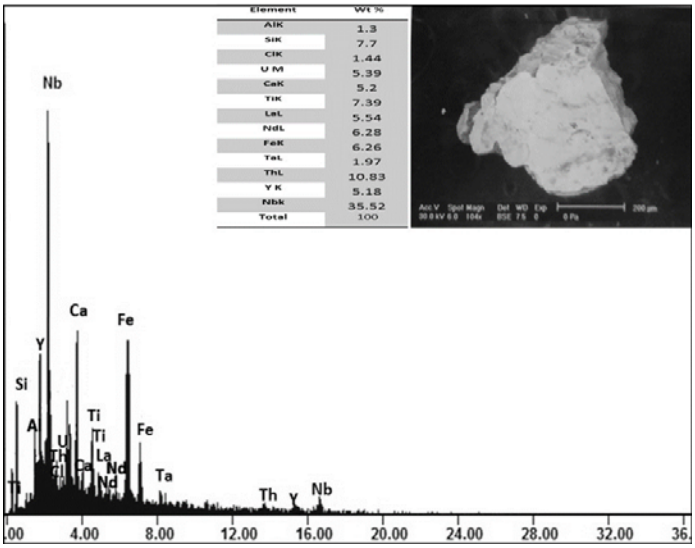

Figure 21. ESEM analyses of samarskite grain, pegmatite.

Monazite[(Ce,La,Y,Th)(PO_4)] is picked up from pegmatite of Gabal Homra. It appears as oval yellow grains with vitreous luster figure 22. The EDX analysis shows the presence of Ce, La, Nd, Pr, Sm, Gd, U, Th and P figure 23.

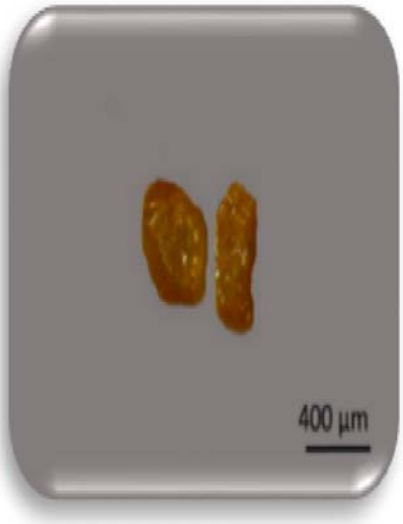

Figure 22. Photomicrograph of monazite grains, pegmatite.

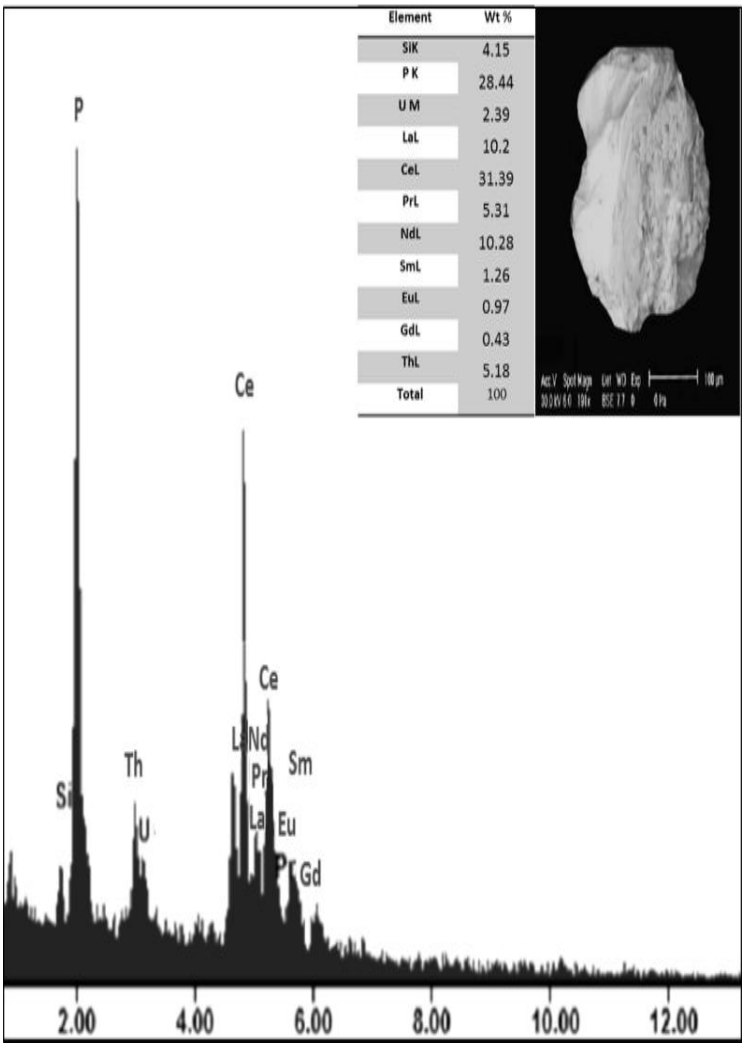

Figure 23. ESEM analyses of monazite grain, pegmatite.

Xenotime[Y (PO_4)] is found as grains in pegmatites. It is uraniferous, brownish in colour, infrequently pleochroic from pale pink to pale yellow, exemplified by short prismatic crystals shape figure 24. The EDX data signify the presence of Y, P, U, Th and REE figure 25.

Xenotime[Y (PO_4)] is found as grains in pegmatites. It is uraniferous, brownish in colour, infrequently pleochroic from pale pink to pale yellow, exemplified by short prismatic crystals shape figure 24. The EDX data signify the presence of Y, P, U, Th and REE figure 25.

Allanite[(Ca, Ce, La)$_2$ (Al, Fe^{3+}, Fe^{2+})$_3$ O. SiO_4. Si_2O_7. OH] occurs in anomalous monzogranite. It forms subhedral to anhedral grains with submetallic luster, varying in colour from brownish black to black figure 26. It is composed of Ce, La, Nd, Y, Sm, Gd, U, Th, Fe, Ca, Al and Si figure 27.

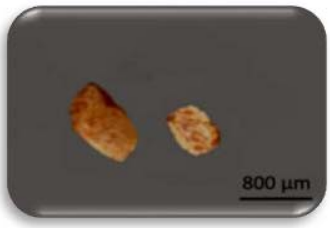

Figure 24. Photomicrograph of xenotime grains, pegmatite.

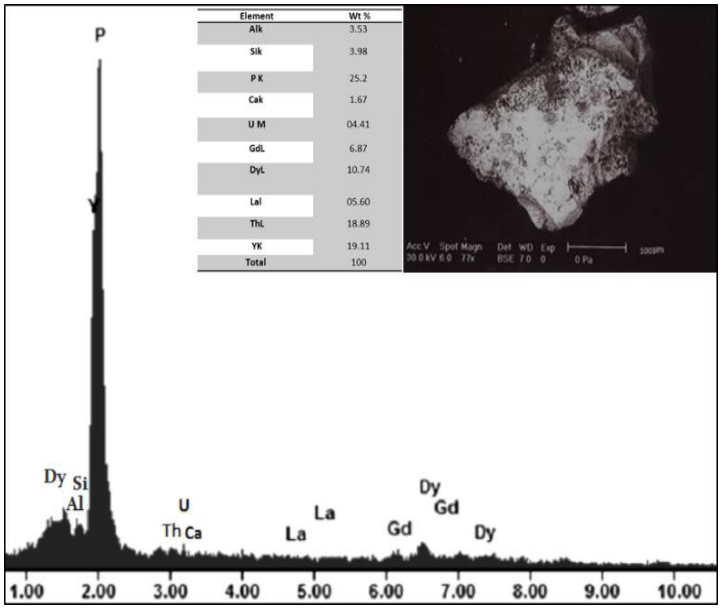

Figure 25. ESEM analyses of xenotime grain, pegmatite**.**

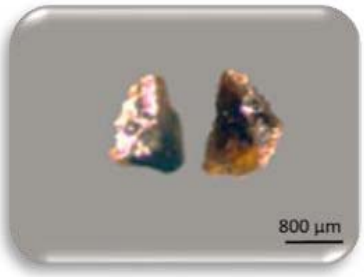

Figure 26. Photomicrograph of allanite grains, anomalous monzogranite.

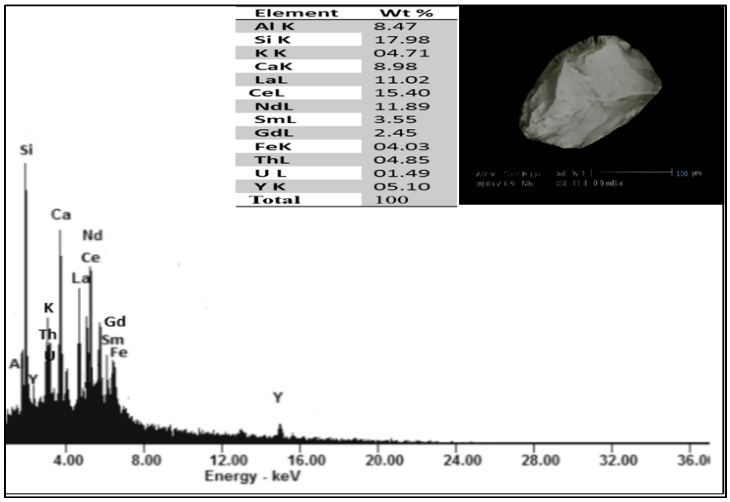

Figure 27. ESEM analyses of allanite grain, anomalous monzogranite.

3.8. Non-radioactive minerals

Pyrite[FeS_2] and hematized pyrite are pick up from both pegmatite and monzogranite. The separated pyrite grains appear as cubic crystals varying in colour from pale brass yellow to brass yellow with metallic luster figure 28A and D. Hematized pyrite appears combining pyrite crystals and broadcasted in the wall rocks mainly along faults and fractures zones figure 28B and C. The X-ray diffraction pattern confirms that the separated pyrite grains are matched with the ASTM card No. (0026-0801) and (0083-0983), figure 28E.

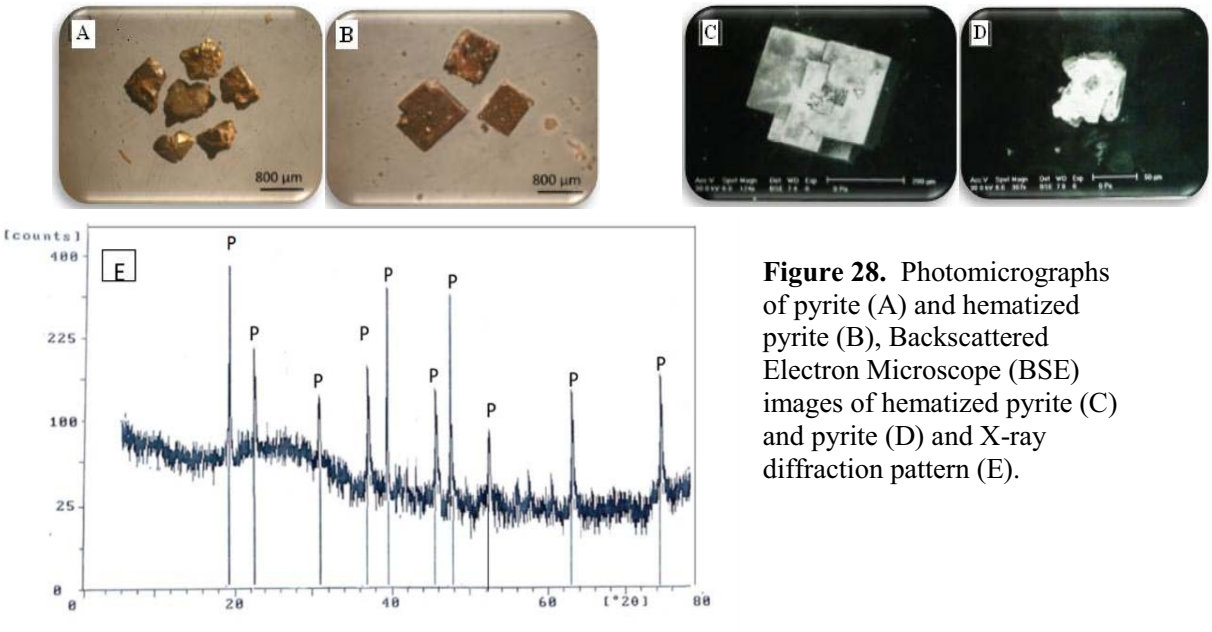

Figure 28. Photomicrographs of pyrite (A) and hematized pyrite (B), Backscattered Electron Microscope (BSE) images of hematized pyrite (C) and pyrite (D) and X-ray diffraction pattern (E).

Goethite [FeO (OH)] is detected in pegmatite and monzogranite as separated massive grains varying in color from dark brown to black and display cloudy luster figure 29A. The X-ray diffraction pattern displays that the goethite grains agree with with the ASTM card No. (0017-0536) and hematite grains agree with the ASTM card No. (0079-0007) figure 29E.

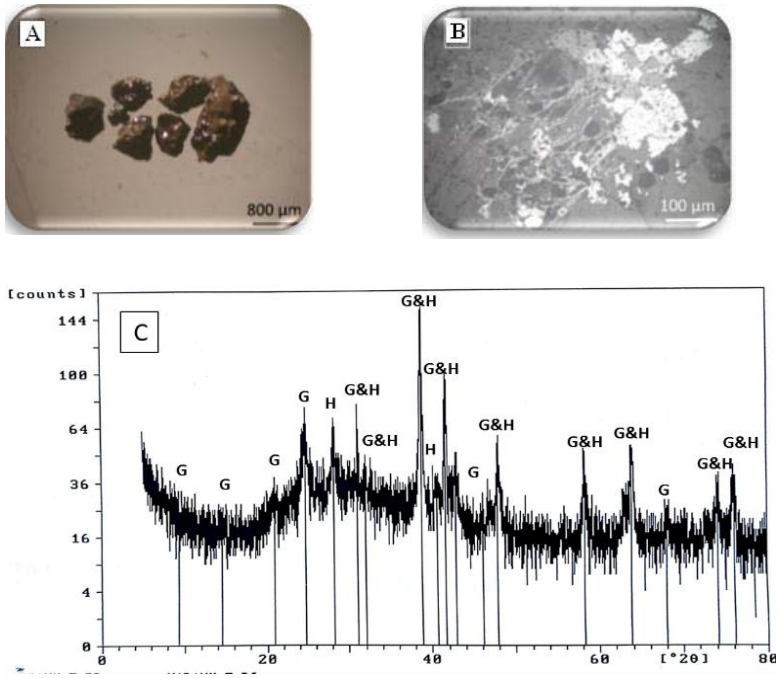

Figure 29. Photomicrograph of geothite (A), microphotograph of hematite and X-ray diffraction pattern (E) for geothite (G) and hematite (H).

Hematite (Fe_2O_3) is found as thin or thick tabular reddish brown crystals of cloudy luster in compact or fibrous form figure 29B. It was recognized by XRD analyses associated with goethite figure 29E.
Magnetite (Fe_3O_4) occurs in both monzogranite and pegmatite. It is partially altered to hematite figure 30A). The X-ray diffraction pattern displays that the magnetite grains agree with the ASTM card No. (0079-0417) and ilmentite grains agree with the ASTM card No. (0003-0741), figure 30C.

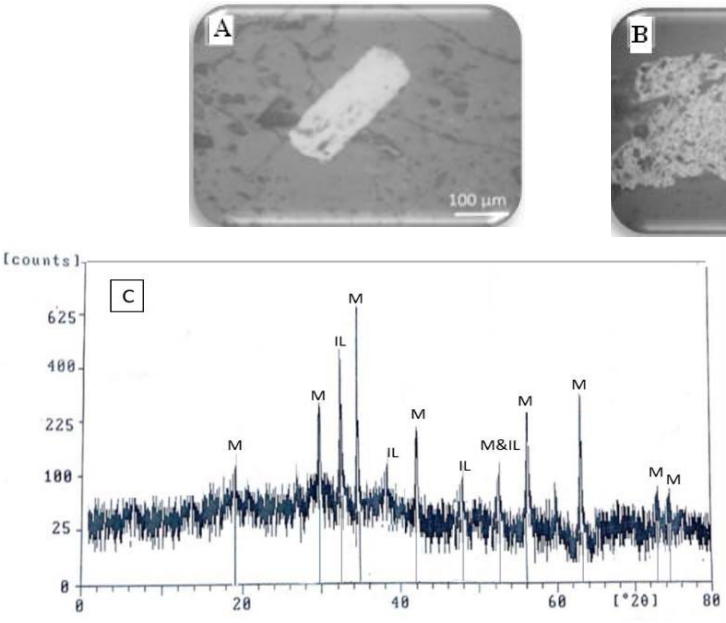

Figure 30. (A) micro-photographs of magnetite (M), (B) ilmenite (IL) and X-ray diffraction pattern (c).

Ilmenite ($FeTiO_3$) is mainly reported as an accessory mineral in the pegmatite, black in colour with metallic luster, unstable Ti-bearing mineral appearing in tabular crystals or platy shape (Figure 30B). This mineral is recognized by XRD pattern associated with magnetite figure 30C. It is predominantly constituted of Fe_2O_3 and TiO_2 with little amounts of Si, Al, U and Mg oxides.
Rutile (TiO_2) differs in colour from yellowish red, red, brown to black colours figure 31A. The EDX records indicates that rutile is essentially composed of Ti, Fe, Nb, Ca, Al and Si figure 31C.

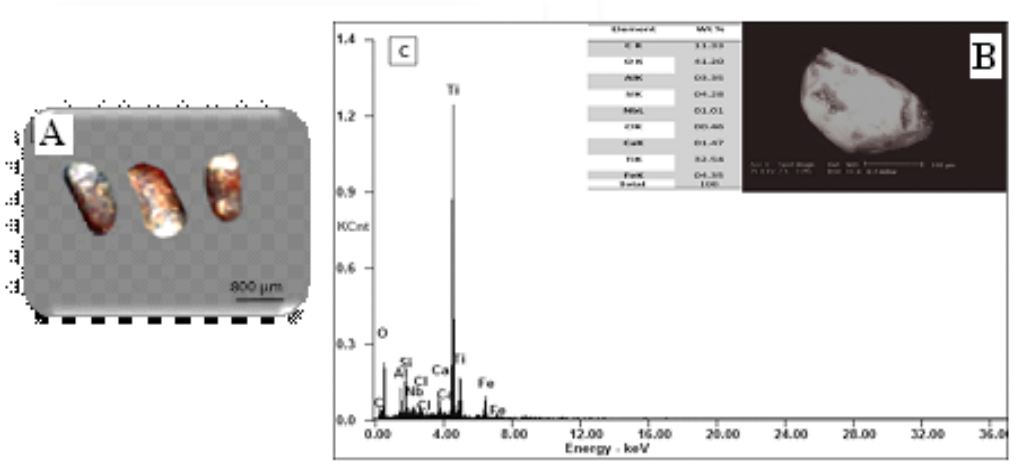

Figure 31. Photomicrograph of rutile (R) grains from pegmatites (A), X-ray diffraction pattern (B) and ESEM analyses (C).

4. Conclusions

Wadi Sabbagh area is situated at southern part of Sinai Peninsula, occupies about 469 Km^2, embodied by moderate and high relief mountains of rugged topography mainly of older and younger granites. The pegmatites broadly distributed in the examined area.

The field radiometric survey indicates that, monzgranites verify the highest values of radioactivity reflecting the role of post-magmatic processes. Two anomalous zones are recognized. The first anomaly confind to the pegmatite bodies hosted in syenogranites. The laboratory radiometric measurements of pegmatites revealed that, the eU reachs up to 168 ppm, while the eTh reachs up to 257 ppm. The average values of Ra and K are 89 ppm and 1.7 wt percentage, respectively. This means that the studied pegmatites are uraniferous. The second anomaly restricted to the anomalous monzogranite at Wadi Adawi area, its eU reachs up to 305 ppm and eTh to 382 ppm. The post magmatic processes could explain the high value of uranium and thorium which lead to the later hydrothermal alteration, which occur mostly along weak planes (fractures, faults and shear districts). The inter-elements variation diagrams recommends that the radioactivity of the concerned rocks most possibly linked to syngenetic and epigenetic foundations. The recognized radioactive minerals in the considered pegmatites are thorite, uranothorite, zircon, fluorite, columbite, samarskite, monazite, xenotime and allanite, whereas thorite, uranothorite, zircon and fluorite are the main radioactive minerals in the altered monzogranite. Additional accessory minerals such as ilmenite, magnetite, hematite, pyrite and rutile were found in the studied pegmatites. Hematite, magnetite and pyrite are the foremost accessories assosciating the radioactive minerals in the monzogranite.

5. References

[1] *Be'eri-Shlevin Y., Katzir Y., Whitehouse M. (2009a):*Post-collisional tectonomagmatic evolution in the northern Arabian-Nubian Shield (ANS): time constraints from ion-probe U–Pb dating of zircon. Journal of Geological Society 166, 71–85.

[2] Abd El Hadi A. Abbas, Mahmoud R. Khattab, Marwa M. Abdel Azeem (2018): Natural radionuclides distribution and environmental impacts of ferruginous sand-siltstone (raw material) and their manufactured Ahmer oxide used as wall paints. Environmental Forensics, 19: 217-224.

[3] Matolin M (1991) Construction and use of spectrometric calibration pads. A report to the Arab republic of Egypt. EGY 4/030-03, Laboratory of Gamma ray spectrometry.

[4] El Nahas, H.A., El Feky, M.G., Mira, H (2011): Mineralogy, M-type tetrad effect and radioactivity of altered granites at the G. Abu Garadi shear zone, central Eastern Desert, Egypt. Chinese journal of Geochemistry, 30, 153- 158.

[5] Khamis, H. A., Ebyan, O. A. and Abed, N. S. (2019): Mineralogy and geochemistry of a new uranium occurrence at the decant of Wadi El Reddah, Northeastern Desert, Egypt. Nuclear Sciences Scientific Journal, in press.

[6] Rogers, J. J. W. and Adams, J. A. S. (1967): "Uranium". In: Wedepohl, K. H. (ed.), Handbook of geochemistry, 2 (1), Springer-Verlag, Berlin.

[7] EL Sayed, A. A. (1993): "Geology and radioactivity of west Dahab area, Southeastern Sinai, Egypt". M. Sc. Thesis, El Mansoura Univ, 174p.

[8] Adams, J. A. S., Osmand, J. K. and Rogers, J. J. W. (1956): "The geochemistry of thorium and uranium. In: Physics and Chemistry of the Earth", 3, pp. 298-348, Pergamon Press, New York.

[9] Ford, K. L. (1982):Uraniferous pegmatites of the sharbot lake area, Ontario; in Uranium in Granites, ed. Y.T.Maurice, Geol. Surv. Can., paper 81-23, p. 125-138.

[10] Moharem, A. F. (2004): Uranium distribution in the Um Samra-Um Bakra granitic plutons and associated pegmatites, Central Eastern Desert, Egypt. 7. Arab Conference on the Peaceful Uses of Atomic Energy, Sana'a (YE). Vol. 1.

[11] Darnely, A. G. (1982): “"Hot granite": Some general remarks”. In Maurice, Y. T. (ed.), Uranium in granites. Geol. Sur. of Canada. Paper 81-23, pp. 1-10.
[12] Sallam, O.R. (2006): Geology and Uranium Potentiality of GabalShiekhEl-Arab Area, South Sinai, Egypt. Ain Shams Univ., Egypt.
[13] Abbas, A. A. (2008): Geology and radioelements distribution in the basement rocks of Wadi Um Adawi area, south Sinai, Egypt. Ph.D. Thesis Ain ShamsUniv., Egypt.
[14] *Charbonneau, B. W. (1982):* “Radiometric study of three radioactive granites in the Canadian Shield: Elliot Lake, Ontario; Fort Smith, Fury and Hecla, NWT. In: Uranium in granites (ed), Y.T.Maurice”. Geol. Surv. Canada, pp. 88-23, pp. 91-99.
[15] El Gharbawy R.I. and El Maadawy W.M. (2012): Geochemistry of the uranium-thurium-bearing granitic rocks and pegmatites of Wadi Haleifiya area, Southeastern Sinai, Egypt. Chin.J.Geochem., 31, 242–259.
[16] El Mezayen, A. M., M. A. Heikal1, El-Feky, M. G., Shahin, H. A., Abu Zeid, I. K., Lasheen1, S. R. (2019): Petrology, geochemistry, radioactivity, and M–W type rare earth element tetrads of El Sela altered granites, south eastern desert, Egypt. Acta Geochim., 38(1), 95–119.